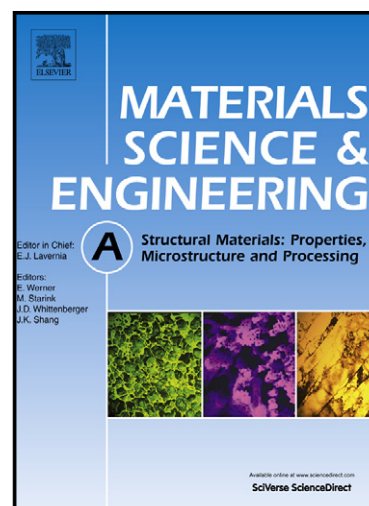# Author's Accepted Manuscript

Constitutive modelling of the flow behaviour of a β titanium alloy at High strain rates and elevated temperatures using the Johnson-cook and modified Zerilli-Armstrong models

Hongyi Zhan, Gui Wang, Damon Kent, Matthew Dargusch

MATERIALS SCIENCE & ENGINEERING A
Structural Materials: Properties, Microstructure and Processing

www.elsevier.com/locate/msea

Cite this article as: Hongyi Zhan, Gui Wang, Damon Kent, Matthew Dargusch, Constitutive modelling of the flow behaviour of a β titanium alloy at High strain rates and elevated temperatures using the Johnson-cook and modified Zerilli-Armstrong models, *Materials Science & Engineering A,* http://dx.doi.org/10.1016/j.msea.2014.06.030

Constitutive modelling of the flow behaviour of a β titanium alloy at high strain rates and elevated temperatures using the Johnson-Cook and modified Zerilli-Armstrong models

Hongyi Zhan[1,*], Gui Wang[1, 2], Damon Kent[1], Matthew Dargusch[1, 2]

[1]Centre for Advanced Materials Processing and Manufacture, School of Mechanical and Mining Engineering, The University of Queensland, St Lucia, Queensland 4072, Australia

[2]Defence Material Technology Centre, Level 2, 24 Wakefield St, Hawthorn VIC 3122, Australia

[*]h.zhan@uq.edu.au

Abstract

The objectives of this work are to characterize the flow behaviour of the Ti-6Cr-5Mo-5V-4Al (Ti6554) alloy at high strain rates and elevated temperatures using the Johnson-Cook (JC) model and a modified Zerilli-Armstrong (ZA) model, and to make a comparative study on the predictability of these two models. The stress-strain data from Split Hopkinson Pressure Bar (SHPB) tests over a wide range of temperatures (293-1173K) and strain rates (10^3-10^4 s^{-1}) were employed to fit parameters for the JC and the modified ZA models. It is observed that both the JC and the modified ZA models have good capacities of describing the flow behaviour of the Ti6554 alloy at high strain rates and elevated temperatures in terms of the average absolute error. The modified ZA model is able to capture the strain-hardening behaviour of the Ti6554 alloy better as it incorporates the coupling effects of strain and temperature. However, dynamic recovery or dynamic recrystallization that may happen at elevated temperatures should be taken into consideration when selecting data set for

parameters fitting for the modified ZA model. Also the modified ZA model requires more stress-strain data for the parameters fitting than the JC model.

Key Words:

β titanium alloys; High strain rate deformation; Johnson-Cook model; Modified Zerilli-Armstrong model

1. Introduction

The usage of the β titanium alloys in the manufacturing of critical load bearing structural parts in the aerospace industry has continued to increase in the past decade owing to their excellent combination of high specific strength, superior fracture toughness and good corrosion resistance. In addition, this category of alloys is deep hardenable through heat treatment processes and has good forgeability which are important features for alloys which are used for manufacturing large section aerospace structures[1-4]. For instance, forgings of Ti-10V-2Fe-3Al (Ti-10-2-3) are increasingly used in the hub of the main rotor system in helicopters and forgings of Ti-5Al-5Mo-5V-3Cr (Ti-5553) have been used for manufacturing landing gear in the Boeing-787 and Airbus-350[5]. Knowledge of materials behaviour at high strain rates and elevated temperatures is necessary for applications such as ballistic impacts in armour applications and materials processing such as machining, hot forging, extrusion etc. Understanding and predicting the behaviour of materials under these extreme conditions is important for a number of fields in engineering including modelling of materials processing and structural behaviour under high strain rate deformation conditions using Finite Element Analysis (FEA). In general, the published information on the flow behaviour of β titanium alloys at high strain rates and elevated temperatures is limited. Therefore, it is important to

evaluate and predict the flow behaviour of β titanium alloys over a wide range of strain rates and temperatures.

Materials constitutive models are used to describe the relationship between flow stress and strain, strain rate and the temperature of materials. This forms the foundation for FEA modelling of the deformation behaviour of materials. Several constitutive models based on different theories have been proposed and can be sorted into three different types: phenomenological, semi-empirical based and physically based models, respectively. Two physically based models: the Mechanical Threshold Stress (MTS) model [6] and the Bammann-Chiesa-Johnson(BCJ) model [7] are based on specific physical theory and are capable of providing good agreement with the experimental results. However, parameters for these two models are difficult to obtain as they always require some data from strictly controlled experimental conditions. In addition, the accuracy of some material property constants used in these physically based models is still in doubt. What's more, these physically based models are not readily available in finite element code. Compared with the physically based models, the Johnson-Cook (JC) model [8], one of the most frequently used empirical models, is preferred by investigators because the parameters for the JC model can be obtained using fewer stress-strain curves due to its simple mathematical form. Also, the JC model can be directly applied to the major commercial finite element packages. In order to improve the accuracy of the JC model, several modifications have been performed including integration of adiabatic temperature rises [9] and microstructural changes [10-12] into the model. The main drawback of the JC model lies in its simple mathematical form as it neglects the coupled effects of strain rate and temperature on the flow stress. Also, being an empirical model the average absolute error will increase with increasing deviation of temperature or strain rate from the reference condition defined by the user [13]. Another frequently used

constitutive model available in finite element code is the Zerilli-Armstrong (ZA) model [14]. Although the ZA model is based on dislocation dynamics, the parameters for the model are still determined by fitting the model to the stress-strain curves of the materials in a similar way to the JC model. Therefore the ZA model is still a form of semi-empirical model. Some researchers prefer the ZA model to the JC model as the former not only incorporates the coupled effects of strain rate and temperature but also considers dislocation characteristics for particular structures. Even though parameters for the ZA model for the Ti6Al4V alloy and different steels [15-22] have been proposed in recent years, some materials constants for the ZA model are very difficult to validate as they require a stress at 0 K and the athermal stress of the materials. Also, it is not valid to use the ZA model for temperatures above half of the melting temperature of the materials [20]. In order to overcome these barriers, Dipti et al. introduced the reference condition into the ZA model and succeeded in using this modified model to predict the mechanical behaviour of a titanium-modified austenitic stainless steel[23] and a modified 9Cr-1Mo steel [24] at low strain rates and elevated temperatures. However, there is still an uncertainty that if this modified version can be used within the high strain rate domain. Therefore further investigations are required to test its applicability.

So far, investigations into the constitutive models for titanium alloys have mainly focused on the Ti6Al4V alloy and several sets of parameters for the JC model have been developed. Very few studies have been concluded on the constitutive model for metastable β titanium alloys. Hokka et.al[25] has obtained one set of parameters for the JC model applied to the metastable beta titanium alloy Ti-15V-3Cr-3Al-3Sn.

The Ti-6Cr-5Mo-5V-4Al (Ti6554) alloy is a newly-developed metastable β alloy with an ultimate tensile strength (UTS) of around 1250MPa and fracture toughness (KIC) from 80 to

90 MPa m$^{1/2}$ after solution and aging treatments [26, 27]. In terms of damage tolerance, the Ti6554 alloy is promising potential for applications in the aerospace industry. The objective of the current study is to evaluate and predict the flow behaviour of the Ti6554 alloy over a wide range of strain rates at elevated temperatures using the JC and modified ZA constitutive models.

2. Experimental procedures

2.1 Sample Preparation

The Ti–6Cr–5Mo–5V–4Al alloy was casted by multiple vacuum arc melting. Ingots of 620 mm diameter were forged to 60% strain at around 1150°C, and then forged with further 70% deformation in the α/β dual phase zone, reducing the diameter to 110 mm. Cylindrical rods with 10 mm in diameter and 80 mm in length were cut by electro discharge machining from the forged ingots. The chemical composition of the alloy is listed in Table 1. Hot rolled cylindrical rods of the Ti6554 alloy were solution treated at 1100 K for 1 h in a protective Argon atmosphere and then air cooled. Aging treatments were conducted on the solution treated Ti6554 rods at 833 K for 8 h under ambient atmosphere and then air cooled. Specimens for microstructural observation were wet ground using silicon carbide papers, mechanically polished and ultrasonically cleaned. Specimens for Optical Microscopy (OM) and Scanning Electron Microscopy (SEM) were etched using Kroll's Reagent (2% hydrofluoric acid, 6% nitric acid and 92% distilled water). SEM was performed on a XL30 instrument. The original microstructure of the Ti6554 alloy, consisting of β phase matrix with α phase precipitates, is shown in Fig.1. Cylindrical specimens with a diameter of 5 mm and length of 4 mm for high strain rate tests were cut from rods using electrical discharge machining with a slow cutting speed to minimise the heat affected zone on the samples. For the tests at a strain rate of 10^4 s^{-1}, a smaller cylindrical specimen with a diameter of 2 mm and

length of 1.5 mm were required due to equipment limitations. As the aspect ratio was maintained, the effect of specimen dimension will not affect the experimental results.

2.2 High Strain Rate Testing

Mechanical behaviour of the Ti6554 alloy at high strain rates was tested using a Split Hopkinson Pressure Bar (SHPB) arrangement at strain rates from $1000s^{-1}$ to $10000s^{-1}$ and temperatures from 293K to 1173K. The SHPB device consists of a striker bar, an input (or incident) bar and an output (or transmitted) bar as shown in Fig.2. The specimen is sandwiched between the input and output bar. Once the striker bar impacts the input bar, a pulse referred to as the incident pulse will be created going through the input bar into the specimen. When the pulse reaches the interface between the input bar and the specimen, part of the pulse (reflected pulse) will be reflected back to the input bar while the rest (transmitted pulse) will be transmitted to the output bar through the specimen. These pulses are recorded by strain gages mounted on the bars. The flow stress σ, strain ε and strain rate $\dot{\varepsilon}$ are then calculated using the following equations:

$$\sigma = E \frac{A_b}{A_s} \varepsilon_t$$

(1)

$$\dot{\varepsilon} = -2 \frac{C_0}{L} \varepsilon_R \qquad (2)$$

$$\varepsilon = -2 \frac{C_0}{L} \int \varepsilon_R dt \qquad (3)$$

ε_R and ε_t represent the reflected pulse and transmitted pulse, respectively. A_b is the cross-sectional area of the bars, A_s is the cross-sectional area of the specimen and L is the gauge length of the specimen. C_0 is the elastic wave speed in the bars which can be calculated by the equation $\sqrt{E/\rho}$ where E and ρ correspond to Young's modulus and the density of the specimen, respectively.

For the experiments at elevated temperatures, the specimens were heated by an in-situ induction coil and the temperature was regulated by a thermocouple not in contact with the specimen. After reaching the designated temperature, the specimen was maintained at the designated temperature for approximately 2 minutes to ensure a uniform temperature

distribution. The incident and transmitted bars were then assembled by a pushing support. The striker bar was launched with the assembly of incident and transmitted bars synchronously to avoid temperature drops in the specimen. The assembly must be completed before the stress wave arrives at the incident bar. The contact time should also be controlled to within 500 ms as the contact between the bars and the specimen will lead to a temperature drop in the specimen. In order to decrease the friction between the contact surfaces of the bars and specimen, molybdenum sulphide was used as a lubricant.

3. Results and discussion

3.1 Flow stress behaviour

Flow curves of the Ti6554 alloy at a range of temperatures (293-1173K) and strain rates (10^3-10^4 s^{-1}) are shown in Fig.3. It could be observed that the flow stress increases with increasing strain rates and decreasing temperatures. Furthermore, flow stress of the Ti6554 alloy is more sensitive to temperature than strain rate. Flow curves at 293K all exhibit a negative strain hardening rate while the strain hardening rate will increase to become positive with increasing temperature, which has been attributed to dynamic strain aging (DSA) caused by the activation of solute Cr atoms in our previous study[28]. The flow curve from the test at 1173K and 4000 s^{-1} in Fig.3 (b) reveals a small peak at a strain of 0.125 followed by a gradual drop of stress towards a plateau, which is the main characteristic of dynamic recrystallization (DRX). This is in accordance with the SEM image shown in Fig.4 (a) in which some DRX grains have been observed. As the β transus of the Ti6554 alloy is around 1023K, α precipitates have been dissolved into the β matrix in the specimens deformed at 1173K as shown in Fig4 (a) and (b). Specimens deformed at high strain rates and temperatures below 873K all exhibit the similar microstructure as shown in Fig.4 (c) in which α phase precipitates cluster inside the β matrix and nucleate along the β grain boundaries. A kind of

string-like α precipitate stretching across some grains has been observed in the samples deformed at strain rates of 4000 s^{-1} and 10000 s^{-1} when the experimental temperature is raised to 873K as shown in Fig.4 (d). This kind of novel α precipitates morphology has been described in detail in our previous study[28]. Though these precipitates of high aspect ratio are supposed to act as barriers to the dislocations movement, no obvious strengthening phenomenon has been observed in flow curves in Fig.3. Hence this microstructural change can be neglected in the constitutive modelling of the flow behaviour of the Ti6654 alloy in order to simplify the establishment of constitutive models.

3.2 Establishment of materials constitutive models

3.2.1 Johnson-Cook model

The basic form of the JC model is defined by the product of three distinctive mathematical terms:

$$\sigma = \left(A + B\epsilon^{n}\right)\left(1 + C\ln\frac{\dot{\epsilon}}{\dot{\epsilon}_0}\right)\left[1 - \left(\frac{T - T_r}{T_m - T_r}\right)^{m}\right] \tag{4}$$

in which σ is the equivalent flow stress, ε is the equivalent plastic strain, $\dot{\epsilon}$ is the equivalent plastic strain rate and $\dot{\epsilon}_0$ is the reference equivalent plastic strain defined by the user (usually defined as 1.0 s^{-1} or 1×10^{-3} s^{-1}). T, T_r and T_m are the workpiece temperature, reference temperature (the minimum temperature under the experiment conditions) and materials melting temperature, respectively. There are five parameters in this model in which A is the yield stress, B and n are used to describe strain hardening effects, C accounts for strain rate hardening and m accounts for thermal softening effects.

The procedures for parameters fitting for the JC model are illustrated below: Taking 293K as the reference temperature and 10^{-3} s^{-1} as the reference strain rate, the dynamic behaviour of the Ti6554 alloy can be represented accurately by the power law equation under the reference condition:

$$\sigma = \left(A + B\epsilon^n \right) \tag{5}$$

The value A is the yield stress under the reference condition (or stress at a strain of 0.002). Then plotting of $\ln(\sigma - A)$ vs. $\ln\epsilon$ gives B from the y-intercept and n from the slope. However, it was observed in our previous study[28] that the flow stress of the Ti6554 alloy tends to increase to a greater degree beyond a strain rate of 10^3 s^{-1}. Therefore a better approach would be to use a higher strain rate, 10^3 s^{-1}, as the reference strain rate. Following the steps above, A, B and n are calculated out to be 1397.5 MPa, -569.47 MPa and 1.215, respectively.

At the reference temperature of 293K with a fixed strain of 0.10, the JC model can be simplified to:

$$\sigma/\sigma_0 = 1 + C\ln\dot{\varepsilon} \tag{6}$$

where σ_0 is the stress at $\dot{\varepsilon} = 1000$ s^{-1}, T=293K and ε=0.10. Using the flow stress at the same temperature and strain but different strain rates to plot the curve $\{(\sigma/\sigma_0)-1\}$ vs. $\ln\dot{\varepsilon}$ gives C from the slope of the curve. C is calculated to be 0.03052 and the results of fitting are shown in Fig.5 (a).

At a strain rate of 4000 s^{-1} with a fixed strain of 0.10, the JC model can be written as:

$$\sigma/\sigma_b = 1 - T^{*m} \tag{7}$$

where σ_b is the stress at $\dot{\varepsilon} = 4000$ s^{-1}, T=293K and ε=0.10. Using flow stress data at the same strain rate and strain but different temperatures to plot a curve of $\ln(1 - \sigma/\sigma_b)$ vs. $\ln T^*$ gives m from the slope of this curve. For high strain rate deformations, it is important to incorporate adiabatic heating into the model. One equation has been extensively used to estimate the temperature elevation during high strain rate deformation:

$$\Delta T = \frac{\eta}{\rho c} \int_{\varepsilon_i}^{\varepsilon_{i+1}} \sigma\left(\varepsilon_i, \dot{\varepsilon}_i, T_i \right) d\varepsilon \tag{8}$$

in which ρ and c are the density and specific heat capacity of the material, respectively. The integral is the plastic work i.e. the area under the stress-strain curve. η is the heat fraction

coefficient. The prevalent perspective is to define η as 0.9 [29-31]. Following the procedures above, m is calculated out to be 0.91 and the fitting results are shown in Fig.5(b).

Parameters for the Ti6554 alloy to suit the JC model are listed in Table.2. They were derived from the data set shown in Fig.5(a) and Fig.5(b). Another five curves performed under different conditions were used to validate the effectiveness of the JC model for the Ti6554 alloy. The comparison between the predicted curves and experimental curves is shown in Fig.5(c). The average absolute error(Δ) is used to assess the fitting results. Δ is defined as :

$$\blacklozenge = \frac{1}{N} \sum_{N}^{i=N} \left| \frac{\sigma_{exp}^{i} - \sigma_{p}^{i}}{\sigma_{exp}^{i}} \right| \times 100 \tag{9}$$

The average absolute error of the fitting results in Fig.5(c) is 6%.

3.2.2 Modified ZA model

The format of the modified ZA model is modified on the basis of the ZA fcc model [23] :

$$\sigma = \left(C_1 + C_2 \varepsilon^n \right) \exp\{ -\left(C_3 + C_4 \varepsilon \right) T^* + \left(C_5 + C_6 T^* \right) \ln \dot{\varepsilon}^* \} \tag{10}$$

$$T^* = T - T_{ref} \tag{11}$$

$$\dot{\varepsilon}^* = \dot{\varepsilon} / \dot{\varepsilon}_{ref} \tag{12}$$

in which σ is the equivalent flow stress, ε is the equivalent plastic strain. $\dot{\varepsilon}$ is the equivalent plastic strain rate and $\dot{\varepsilon}_{ref}$ is the reference equivalent plastic strain defined by user. T and T_{ref} are the workpiece temperature and reference temperature, respectively. C_1, C_2, C_3, C_4, C_5, C_6 and n are seven parameters of the modified ZA model. The rationale for the modifications to the ZA model were described in detail in [23] and [24]. The procedures to determine the parameters for the modified ZA model are illustrated below:

A strain rate of 1000 s^{-1} and temperature of 293K were used as the reference strain rate and temperature due to the same reason stated in Section 3.2.1 for the Johnson-Cook model. Under the reference condition, the modified ZA model can be simplified to:

$$\sigma = C_1 + C_2\varepsilon^n \tag{13}$$

C_1 represents the yield stress under the reference condition with C_2 and n accounting for the effects of strain hardening on the flow stress. Then plotting the curve $\ln(\sigma-C_1)$ vs. $\ln\varepsilon$ gives C_2 and n from the y-intercept and slope of the curve, respectively.

Then at the reference strain rate, Eq.(10) can be simplified to :

$$\sigma = \left(C_1 + C_2\varepsilon^n\right)\exp\left[-\left(C_3 + C_4\varepsilon\right)T^*\right] \tag{14}$$

Taking the natural logarithm of Eq.(14), it can be expressed as:

$$\ln\sigma = \ln\left(C_1 + C_2\varepsilon^n\right) - \left(C_3 + C_4\varepsilon\right)T^* \tag{15}$$

$$S_1 = C_3 + C_4\varepsilon \tag{16}$$

S_1 descirbes thermal softening effect and C_4 is used to quantify the influence of strain on the thermal softening effect. S_1 can be obtained by the slope of the curve $\ln\sigma$ vs. T^*. It is found that the slope of the curve $\ln\sigma$ vs. T^*, S_1, becomes smaller as shown in Fig.6 (a) when the data from the testing at 1173K is involved in the fitting. Plotting the curve S_1 vs. ε gives C_3 and C_4 from the y-intercept and slope of the curve, respectively. By plotting the curve S_1 vs. ε it is found that S_1 decreases much slower with increasing strains (0.05-0.15 in steps of 0.025), as shown in Fig.6 (b), when the data from the test at 1173K is included in the parameters fitting. Considering this difference, it is necessary to clarify the influence of the data set selected for the parameters fitting on the predictablility of the modified ZA model.

By taking the natural logarithm of Eq.(10) at a fixed strain, we can get:

$$\ln\sigma = \ln\left(C_1 + C_2\varepsilon^n\right) - \left(C_3 + C_4\varepsilon\right)T^* + \left(C_5 + C_6 T^*\right)\ln\dot{\varepsilon}^* \tag{17}$$

$$S_2 = C_5 + C_6 T^* \tag{18}$$

S_2 quantifies the strain rate hardening effect and it can be obtained from the slope of the curve $\ln\sigma$ vs. $\dot{\varepsilon}^*$. Plotting the curve S_2 vs. ε gives C_5 and C_6 from the y-intercept and slope of the curve.

Two sets of parameters for the modified ZA model for the Ti6554 alloy have been obtained in Table 3 and Table 4. Fitting results using parameters in Table 3 and Table 4 are shown in Fig.7 and Fig.8, respectively. When the data from tests at 1173K is included in the parameters fitting, the agreement between the predicted data and experimental data is poor as shown in Fig.7. When the data from tests at 1173K is excluded, a much better agreement was observed as shown in Fig.8. A large deviation between the experimental data and calculated data in Fig.8 is only observed at strains larger than 0.125 under the conditon of 4000/s and 1173K. This can be attributed to the dynamic recrystallization observed in Fig.4 (a), which cannot be predicted by the modified ZA model. In terms of the fitting results, parameters in Table 4 should be selected to verify the effectiveness of the modified ZA model.

As the parameters in Table 4 were derived from the data set shown in Fig.7 and Fig.8, another three stress-strain curves performed under different conditions were employed to validate the reliability of the modified ZA model. A good agreement has been achieved between experimental data and calculated data as shown in Fig.9. The average absolute error(Δ) of the fitting results in Fig.9 is 5.7%.

3.3 Discussion

One of the main characteristics of the strain hardening behaviour of the Ti6554 alloy at high strain rates over a wide range of temperatures is that flow curves show a negative slope at 293K but the strain hardening rate will increase to become positive with increasing temperature. Both the JC model and the modified ZA model are capable of predicting the

dynamic flow behaviour of the Ti6554 alloy at high strain rates and elevated temeperatures in terms of the average absolute error. However, the modified ZA model is able to give a much better description of the strain-hardening behaviour of the Ti6554 alloy than the JC model.

For the JC model, all the predicted curves maintain a negative slope following the curve performed under the reference condition as shown in Fig.5. This can be explained by the format of the strain hardening rate derived from the JC model:

$$\mathrm{d}\sigma / \mathrm{d}\varepsilon = \left(Bn\epsilon^{n-1}\right)\left(1+C\ln\frac{\dot{\varepsilon}}{\dot{\varepsilon_0}}\right)\left[1-\left(\frac{T-T_r}{T_m-T_r}\right)^m\right] \qquad (19)$$

The sign of the strain hardening rate, $\mathrm{d}\sigma/\mathrm{d}\varepsilon$, is only determined by parameters B and n which are derived from the stress-strain curve under the reference condition. Therefore the sign of $\mathrm{d}\sigma/\mathrm{d}\varepsilon$ will not change with strain, strain rate or temperature. It is also reported that in the JC model the strain-hardening rate will increase with increasing strain rate but decrease with increasing temperatures[16]. In general, the JC model is inadequate to capture the complex strain hardening behaviour of the Ti6554 alloy. It is also found that the prediction of the JC model is particularly satisfactory when the strain is near to 0.10 which is the fixed strain in the fitting of parameters C and m for the JC model. However, the average absolute error of the fitting results in Fig.5 (c) gradually increases with increasing deviation of strain from 0.10 as shown in Fig.10. This indicates that the JC model is only capable of predicting the dynamic flow behaviour of materials very accurately in a narrow domain near the specific strain which is fixed in the parameters fitting for the JC model. In addition, the parameters C and m for the JC model have been reported to be dependent on the strain that is fixed in the parameters fitting process[13].

The modified ZA model has a better capacity to capture the strain hardening behaviour of the Ti6554 alloy at high strain rates as it incorporates the coupling effects of strain and

temperature on the flow stress. The format of $d\ln\sigma/d\varepsilon$ can be derived from the modified ZA model i.e. Eq.(10):

$$d\ln\sigma/d\varepsilon = d\ln\left(C_1 + C_2\varepsilon^n\right) - C_4T^*$$ (20)

According to Eq. (20), the negative sign of C_4 in Table 3 and Table 4 implies that the strain hardening rate will increase with increasing temperature. Comparing parameters in Table 3 with those in Table 4, it is found that a significant difference between these two sets of parameters is that the absolute value of C_4 decreases from 2.22×10^{-3} in Table 4 to 5.2×10^{-4} in Table 3. This indicates that the poor agreement between the predicted and experimental data in Fig.7 is caused by the reduction of C_4. This reduction of C_4 in Table 3 should be caused by the almost zero slope of the flow curve from the test at 1173K. This drop of strain hardening rate at 1173K may be attributed to dynamic recovery or dynamic recrystallization that happen at elevated temperatures. This indicates that when selecting data set for parameters fitting for the modified ZA model, temperature range should be taken into consideration in order to eliminate the influence of dynamic recovery or dynamic recrystallization on the modelling of strian hardening behaivour.

It should also be kept in mind that the JC model only has 5 parameters to evaluate while the modified ZA model has 7. In addition, the modified ZA model requires more experimental data for parameters fitting than the JC model.

4. Conclusions

Original Johnson-Cook (JC) model and a modified Zerilli-Armstrong (ZA) model have been established to characterize the flow behaviour of the Ti6554 alloy over a wide range of strain rates $(10^3\text{-}10^4\ \text{s}^{-1})$ and temperatures (293K-1173K), respectively. Based on this study, following are the conclusions:

1. The main characteristic of the flow behaviour of the Ti6554 alloy at high strain rates is that flow curves exhibit a negative strain hardening rate at 293K while the strain hardening rate will increase to become positive with increasing temperature. The formation of string-like α precipitate can be neglected in the constitutive modelling process as it does not induce extra strengthening effects.

2. The JC model is capable of predicting the dynamic flow behaviour of materials accurately in a narrow domain near the strain value which is fixed in the parameters fitting for the JC model. However the format of the JC model is inadequate to track the complex strain-hardening behaviour of the Ti6554 alloy.

3. The modified ZA model has a much better capacity of describing the strain-hardening rate of the Ti6554 alloy as it incorporate the coupled effects of strain and temperature. However, the temperature range should be controlled when selecting data for parameters fitting for the modified ZA model in order to eliminate the influence of dynamic recovery or dynamic recrystallization.

Reference

[1] R. Boyer, R. Briggs, J Mater Eng Perform, 14 (2005) 681-685.
[2] R.R. Boyer, Advanced Performance Materials, 2 (1995) 349-368.
[3] C. Leyens, M. Peters, Titanium and titanium alloys, Wiley Online Library, 2003.
[4] S. Nyakana, J. Fanning, R. Boyer, J Mater Eng Perform, 14 (2005) 799-811.
[5] N.G. Jones, R.J. Dashwood, D. Dye, M. Jackson, Mat Sci Eng a-Struct, 490 (2008) 369-377.

[6] P.S. Follansbee, U.F. Kocks, Acta Metallurgica, 36 (1988) 81-93.

[7] Y.B. Guo, Q. Wen, M.F. Horstemeyer, Int J Mech Sci, 47 (2005) 1423-1441.

[8] G.R. Johnson, W.H. Cook, in: Proceedings of the 7th International Symposium on Ballistics, The Hague, Netherlands: International Ballistics Committee, 1983, pp. 541-547.

[9] W.-S. Lee, C.-F. Lin, Materials Science and Engineering: A, 241 (1998) 48-59.

[10] S. Seo, O. Min, H. Yang, Int J Impact Eng, 31 (2005) 735-754.

[11] M. Sima, T. Ozel, Int J Mach Tool Manu, 50 (2010) 943-960.

[12] M. Calamaz, D. Coupard, F. Girot, Int J Mach Tool Manu, 48 (2008) 275-288.

[13] D. Samantaray, S. Mandal, A.K. Bhaduri, Comp Mater Sci, 47 (2009) 568-576.

[14] F.J. Zerilli, R.W. Armstrong, J Appl Phys, 61 (1987) 1816-1825.

[15] H.W. Meyer, D.S. Kleponis, Int J Impact Eng, 26 (2001) 509-521.

[16] R. Liang, A.S. Khan, Int J Plasticity, 15 (1999) 963-980.

[17] W.-S. Lee, C.-Y. Liu, Materials Science and Engineering: A, 426 (2006) 101-113.

[18] S.-T. Chiou, W.-C. Cheng, W.-S. Lee, Materials Science and Engineering: A, 392 (2005) 156-162.

[19] D.A.S. Macdougall, J. Harding, J Mech Phys Solids, 47 (1999) 1157-1185.

[20] A. Lennon, K. Ramesh, Int J Plasticity, 20 (2004) 269-290.

[21] S. Dey, T. Børvik, O. Hopperstad, M. Langseth, Int J Impact Eng, 34 (2007) 464-486.

[22] D. Macdougall, J. Harding, J Mech Phys Solids, 47 (1999) 1157-1185.

[23] D. Samantaray, S. Mandal, U. Borah, A. Bhaduri, P. Sivaprasad, Materials Science and Engineering: A, 526 (2009) 1-6.

[24] D. Samantaray, S. Mandal, A. Bhaduri, Comp Mater Sci, 47 (2009) 568-576.

[25] M. Hokka, T. Leemet, A. Shrot, M. Baeker, V.T. Kuokkala, Mat Sci Eng a-Struct, 550 (2012) 350-357.

[26] Y.L. Yang, W.Q. Wang, F.L. Li, Y.Q. Zhang, H.L. Yang, P.H. Zhang, in: Materials science forum, Trans Tech Publ, 2009, pp. 173-176.

[27] Y.Q. Wang, G. Wang, W.Q. Wang, D. Kent, M.S. Dargusch, in: Materials science forum, Trans Tech Publ, 2011, pp. 29-32.

[28] H. Zhan, D. Kent, G. Wang, M.S. Dargusch, Materials Science and Engineering: A, 607 (2014) 417-426.

[29] M. Sasso, G. Newaz, D. Amodio, Mat Sci Eng a-Struct, 487 (2008) 289-300.

[30] W.S. Lee, T.H. Chen, C.F. Lin, N.W. Lee, Mater Sci Tech-Lond, 26 (2010) 1079-1087.

[31] S. Nemat-Nasser, W.G. Guo, V.F. Nesterenko, S.S. Indrakanti, Y.B. Gu, Mech Mater, 33 (2001) 425-439.

Table 1

Chemical composition (wt. %) of the Ti6554 alloy

Materials	Cr	Mo	V	Al	O	Ti
Ti6554	6.05	4.95	5.09	4.20	0.19	Bal

Table 2

Parameters of Ti6554 for the JC model

| JC model parameter	A(MPa)	B(MPa)	n	C	m
Value	1397.5	-569.47	1.215	0.03052	0.91

Table 3

Parameters for the modified ZA model for Ti6554 with data at 1173K included in fitting process

Parameter	C_1(MPa)	C_2(MPa)	n	C_3	C_4	C_5	C_6
Value	1397.5	-569.47	1.215	0.00113	-5.2×10^{-4}	0.03131	-3.12×10^{-5}

Table 4

Parameters for the modified ZA model for Ti6554 with data at 1173K excluded in fitting process

Parameter	C_1(MPa)	C_2(MPa)	n	C_3	C_4	C_5	C_6
Value	1397.5	-569.47	1.215	0.0012	-0.00222	0.03136	-3.21×10^{-5}
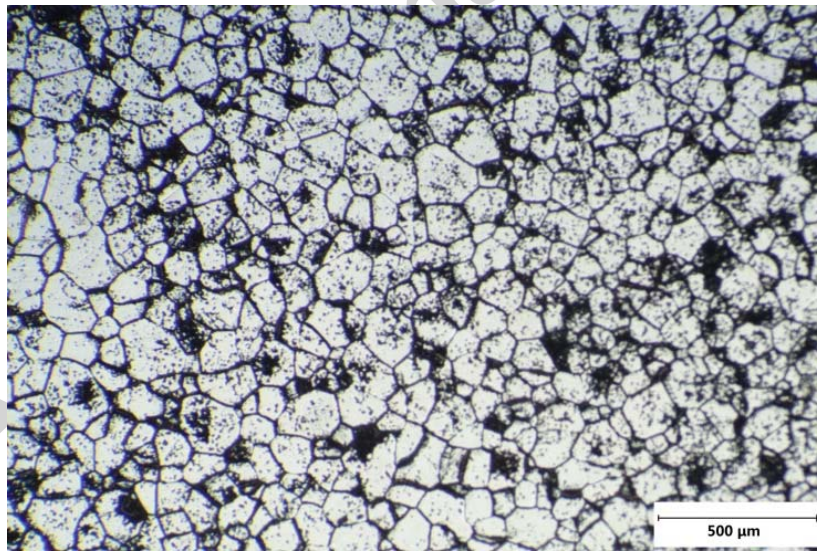
Fig.1. Optical micrograph of the initial microstructure of the Ti6554 alloy
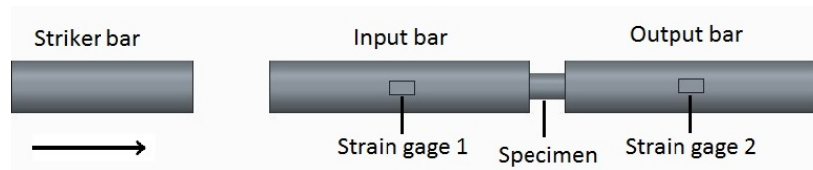
Fig.2. Schematic showing the arrangement of the SHPB device.
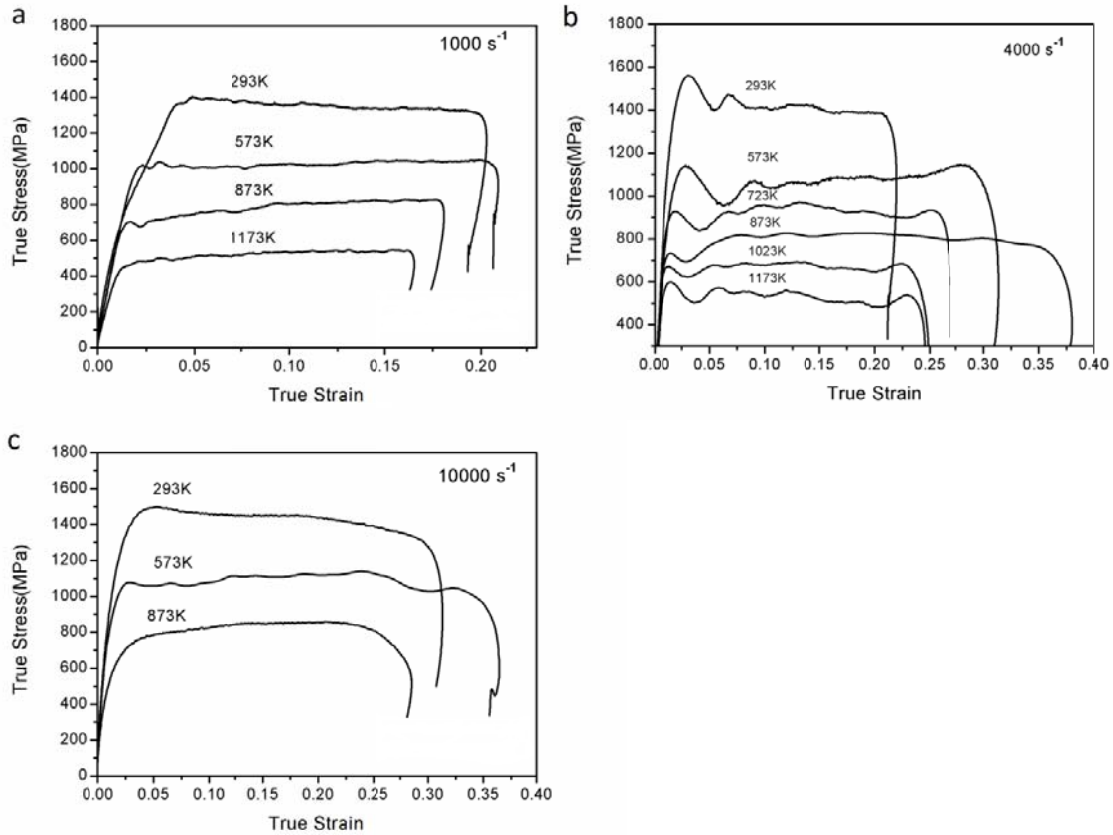
Fig.3. True stress-strain curves of the Ti6554 alloy at various temperatures with strain rate of (a) 1000 s^{-1} (b) 4000 s^{-1} (c) 10000 s^{-1}
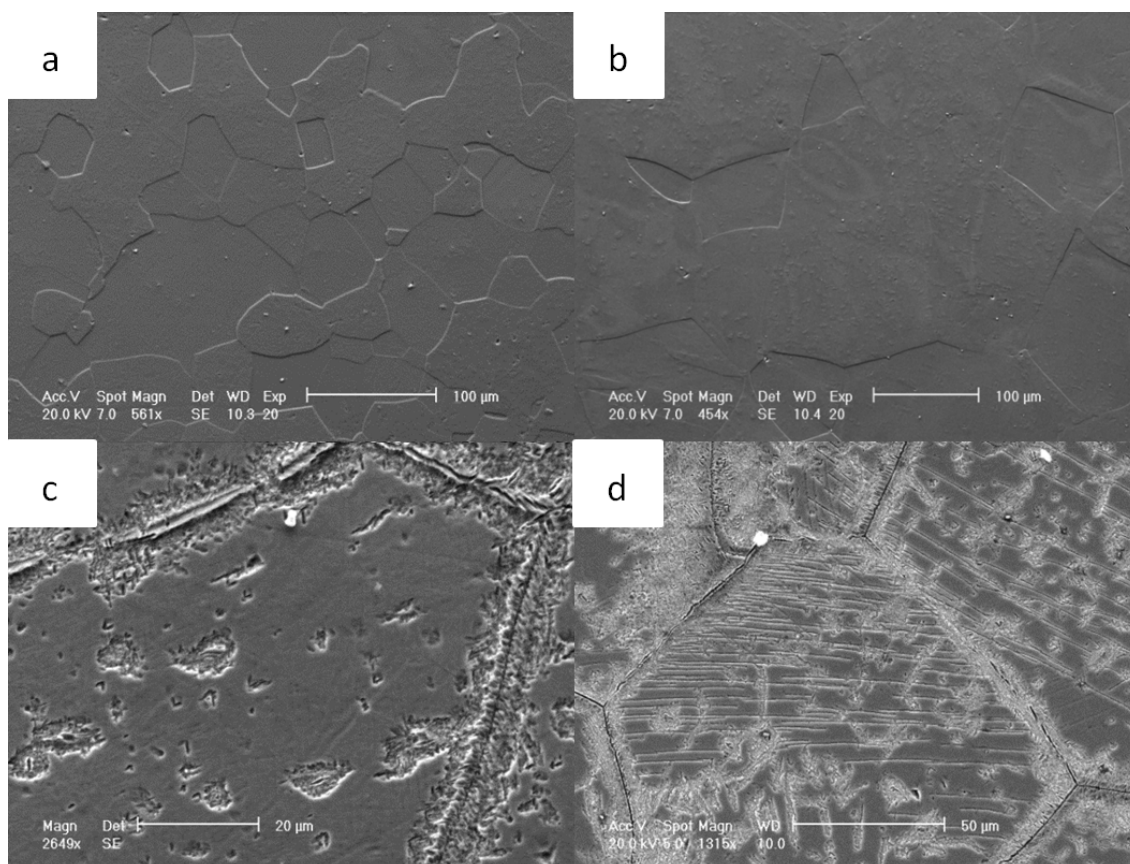
Fig.4. SEM images of samples deformed at**:** (a) 4000 s^{-1}, 1173K; (b) 1000s^{-1}, 1173K; (c) 4000 s^{-1}, 293K; (d) 4000 s^{-1}, 873K.
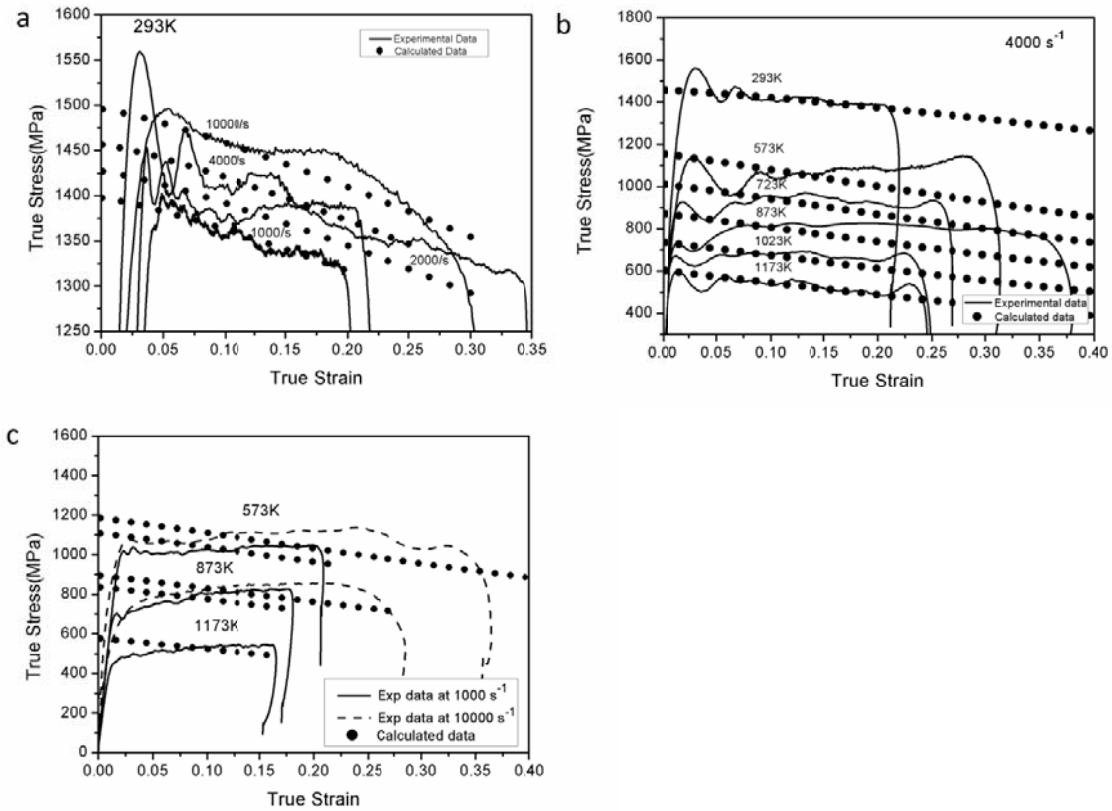
Fig.5. Fitting results using the JC model at (a) 293K (b) 4000 s^{-1}, (c) Validation of the predictability of the JC model
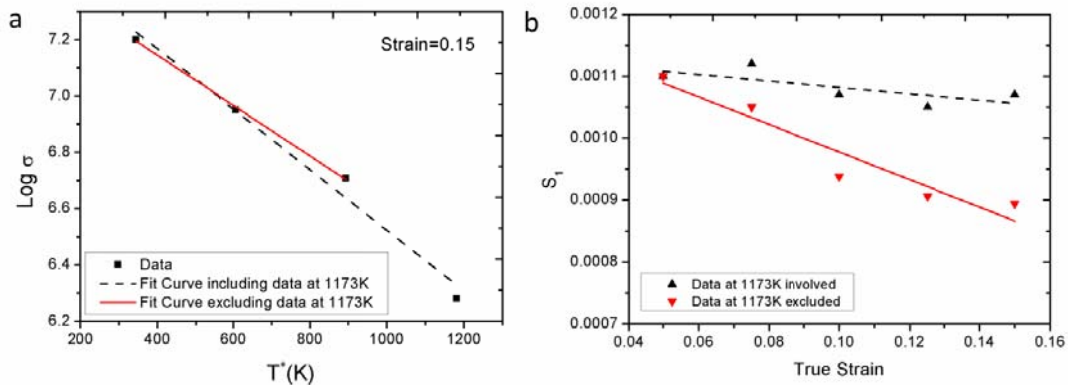
Fig.6. (a) Relationship of logarithmic stress with T* at a strain of 0.15 (b) Relationship of S$_1$ with true strain (0.05-0.15 in steps of 0.025).
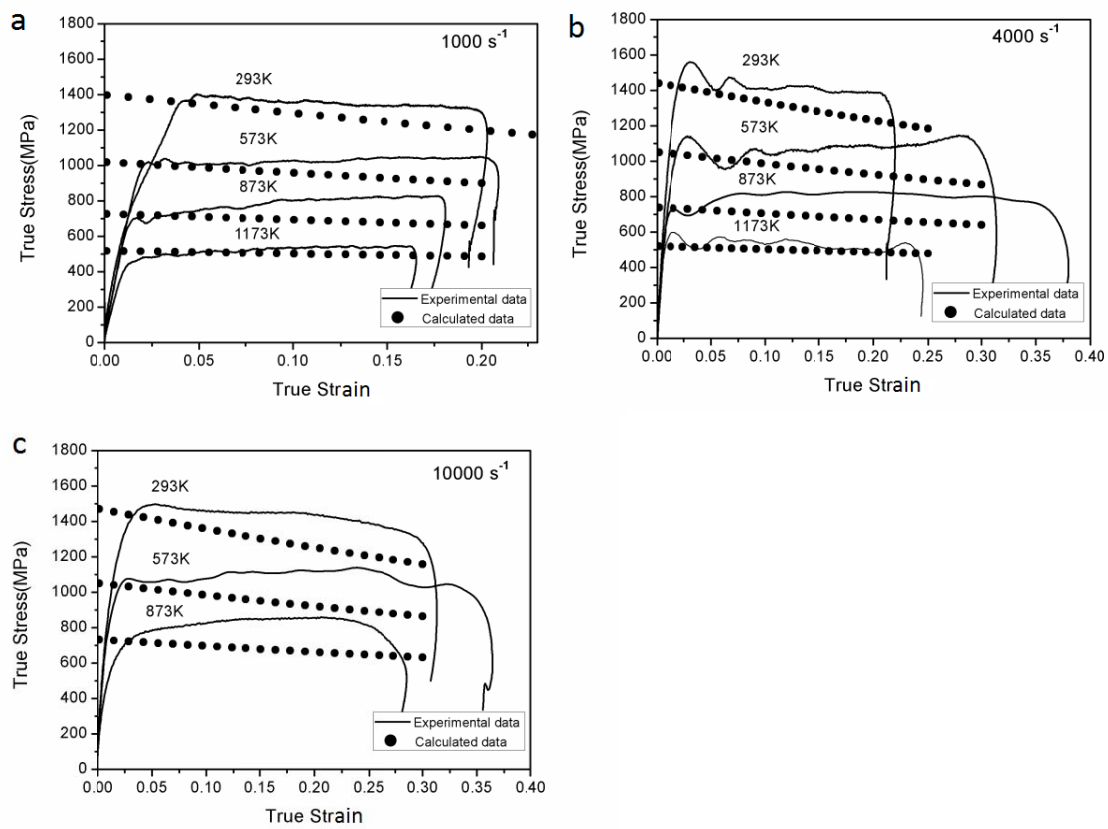
Fig.7. Fitting results using parameters for the modified-ZA model in Table 4: (a) 1000 s^{-1} (b) 4000 s^{-1} (c) 10000 s^{-1}
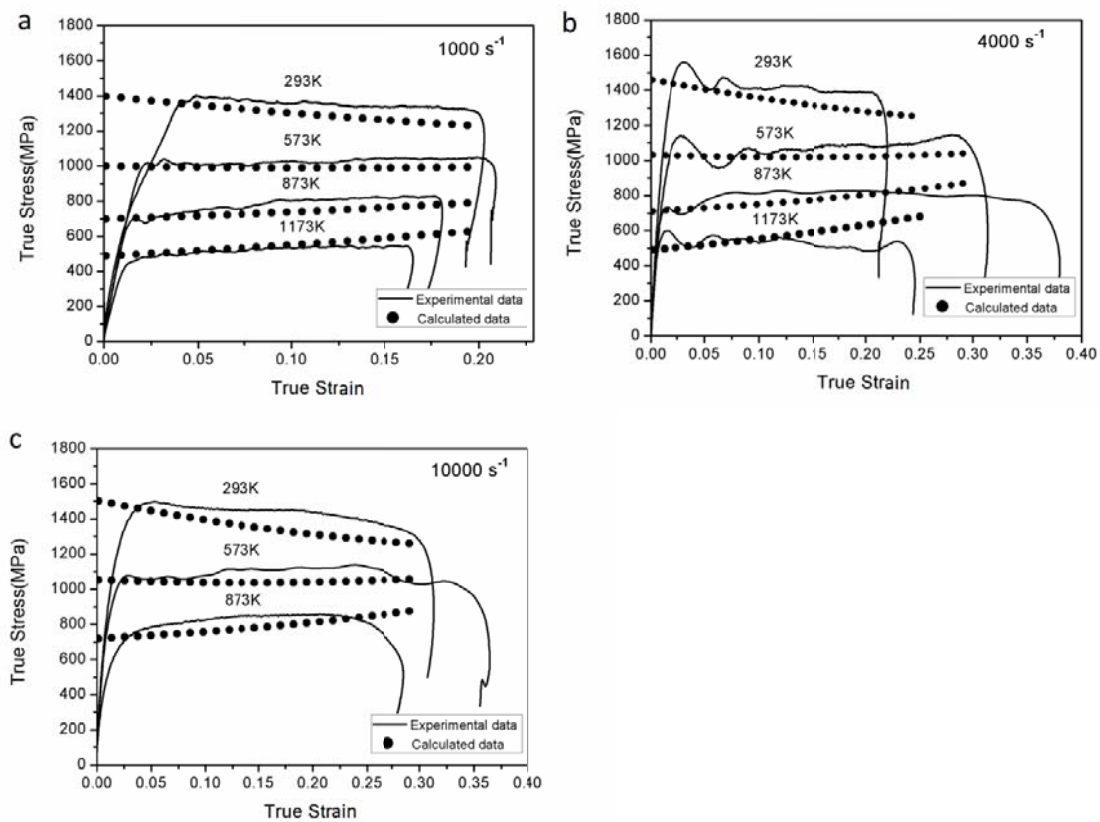
Fig.8. Fitting results using parameters for the modified-ZA model in Table 5: (a) 1000 s^{-1} (b) 4000 s^{-1} (c) 10000 s^{-1}
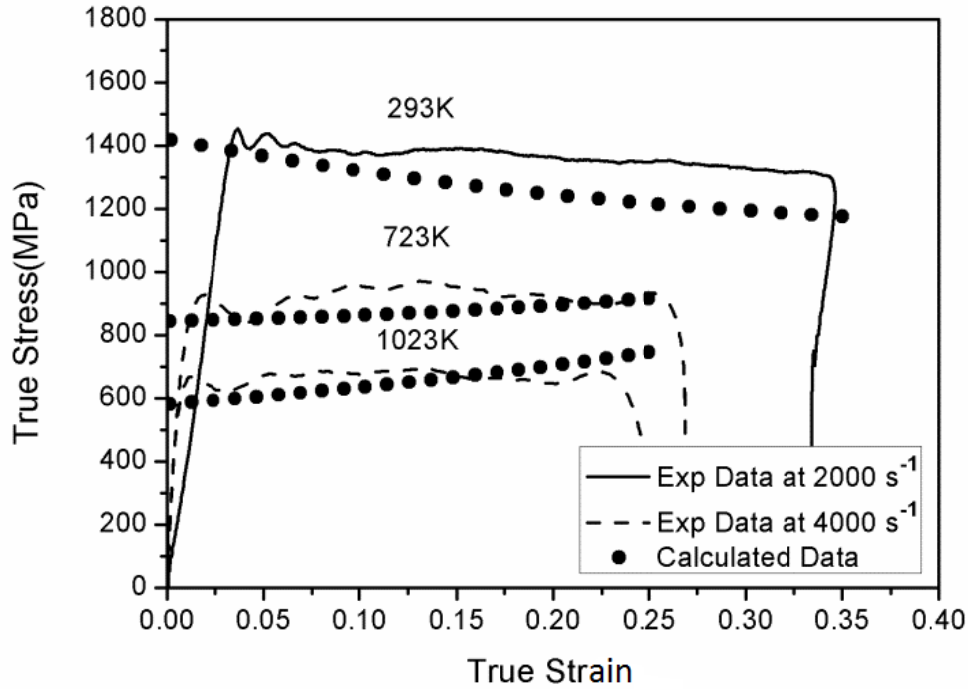
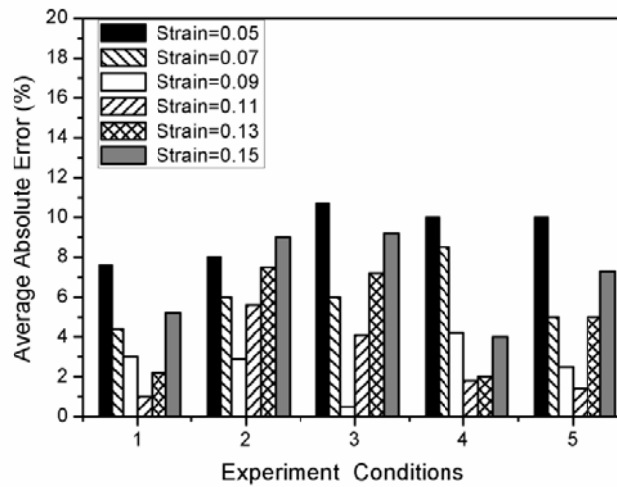**Fig.9.** Validation of the predictability for the modified ZA model.

Fig.10. Variation of average absolute error with strains using the JC model: (1)10^3 s^{-1} 573K; (2)10^3 s^{-1}, 873K; (3)10^3 s^{-1},1173K; (4)10^4 s^{-1},573K; (5)10^4 s^{-1},873K.